https://doi.org/10.5194/egusphere-2023-1223
Preprint. Discussion started: 10 July 2023

Measurement Report: Exchange Fluxes of HONO over Agricultural Fields in the North China Plain

Yifei Song[1,3,#], Chaoyang Xue[2,#,*], Yuanyuan Zhang[1,3,*], Pengfei Liu[1,3], Fengxia Bao[2], Xuran Li[4], Yujing Mu[1,3,*]

[1] Research Center for Eco-Environmental Sciences, Chinese Academy of Sciences, Beijing 100085, China

[2] Max Planck Institute for Chemistry, Mainz 55128, Germany

[3] University of Chinese Academy of Sciences, Beijing 100049, China

[4] Rural Energy and Environment Agency, Ministry of Agriculture and Rural Affairs, Beijing 100125, China

[#] These authors contributed equally to this work.

Correspondence:

Chaoyang Xue (ch.xue@mpic.de)

Yuanyuan Zhang (yyzhang@rcees.ac.cn)

Yujing Mu (yjmu@rcees.ac.cn)

https://doi.org/10.5194/egusphere-2023-1223
Preprint. Discussion started: 10 July 2023

Abstract

Nitrous acid (HONO) is a crucial precursor of tropospheric hydroxyl radicals but its sources are not fully understood. Soil is recognized as an important HONO source, but the lack of measurements of soil-atmosphere HONO exchange flux (F_{HONO}) has led to uncertainties in modeling its atmospheric impacts and understanding the reactive nitrogen budget. To address this, we conduct long-period F_{HONO} measurements over agricultural fields under fertilized ($F_{HONO-NP}$) and non-fertilized ($F_{HONO-CK}$) treatments. Our results show that nitrogen fertilizer use causes a remarkable increase in $F_{HONO-NP}$ and it exhibits distinct diurnal variations, with an average noontime peak of 152 ng N m^{-2} s^{-1}. The average $F_{HONO-NP}$ within three weeks after fertilization is 97.7 ± 8.6 ng N m^{-2} s^{-1}, around two orders of magnitude higher than before fertilization, revealing the remarkable promotion effect of nitrogen fertilizer on HONO emissions.

We also discuss other factors that influence soil HONO emissions, such as meteorological parameters and soil properties/nutrients. Additionally, we estimate the HONO emission factor of 0.68 ± 0.07% relative to the applied nitrogen during the whole growing season of summer maize. Accordingly, the fertilizer-induced soil HONO emission is estimated to be 0.06 and 0.16 Tg N yr^{-1} in the North China Plain (NCP) and China, respectively, representing a significant reactive nitrogen source. Furthermore, our observations reveal that soil emissions sustain a high level of daytime HONO, enhancing the atmospheric oxidizing capacity and aggravating O_3 pollution in the NCP. Our results indicate that in order to effectively mitigate regional air pollution, future policies should consider reactive nitrogen emissions from agricultural soils.

Keywords

HONO; Agriculture fields; Nitrogen fertilizer; North China Plain; Reactive nitrogen budget; Air pollution

1 Introduction

Hydroxyl radical (OH) is the major oxidant in the troposphere, which can oxidize primary pollutants (volatile organic compounds, NO_X, SO_2, etc.), with the formation of

https://doi.org/10.5194/egusphere-2023-1223
Preprint. Discussion started: 10 July 2023

secondary pollutants (aerosols, O_3, etc.). It also determines the lifetime of some greenhouse gases like methane, which affects global climate (Seinfeld and Pandis, 2016). It is therefore necessary to understand the OH formation path. Nitrous acid (HONO) is an important primary OH source, with a contribution of 20–90% to primary OH production in the lower troposphere (Kim et al., 2014; Song et al., 2022b; Tan et al., 2017; Tan et al., 2018; Xue et al., 2020). However, the source of HONO is still incompletely understood, especially during daytime (Jia et al., 2020; Kleffmann et al., 2003; Li et al., 2018; Xue et al., 2022b). Recently, unexpectedly high HONO concentrations up to ppbv level were observed during daytime, suggesting strong daytime missing sources of 0.1–4.9 ppbv h^{-1} in urban and rural areas (Kleffmann et al., 2003; Li et al., 2012; Li et al., 2014; Spataro et al., 2013; Su et al., 2008). In addition, several previous studies have reported significant gradients in vertical HONO distribution, indicating a strong HONO source at the ground surface (Kleffmann et al., 2003; Vandenboer et al., 2013; Wong et al., 2012; Zhang et al., 2009). Among daytime HONO sources, the ground-derived HONO sources mainly include (1) photo-enhanced heterogeneous reaction of NO_2 on the soil surface (George et al., 2005; Han et al., 2016; Stemmler et al., 2006; Stemmler et al., 2007), (2) photolysis of adsorbed nitric acid (Zhou et al., 2011) on the ground surface, (3) release of adsorbed HONO from strong acid (HCl, HNO_3, etc.) displacement (Vandenboer et al., 2015) and (4) soil emissions from biogenic progress, which is considered as an important daytime HONO source in agricultural areas and has been proved by many laboratory experiments and several field flux measurements (Oswald et al., 2013; Su et al., 2011; Tang et al., 2019; Xue et al., 2019a). Under laboratory conditions, Oswald et al. (2013) found that soil mineral nitrogen is substantially associated with HONO emissions, which suggests nitrogen fertilizer use can greatly enhance the potential of soil HONO emissions. In our recent study, elevated levels of HONO concentration and HONO-to-NO_2 ratios were observed after fertilization at an agricultural site, implying that fertilized fields released a great amount of HONO (Xue et al., 2021). To study the characteristics and the corresponding

https://doi.org/10.5194/egusphere-2023-1223
Preprint. Discussion started: 10 July 2023

atmospheric impacts of soil HONO emissions, it is necessary to conduct direct flux measurements.

Flux measurement can provide direct evidence about the production and/or deposition of HONO on the ground surface (Von Der Heyden et al., 2022; Xue et al., 2022a). There are two types of methods to measure HONO exchange flux between soil and atmosphere: micrometeorology and chamber methods. The micrometeorology methods include the eddy covariance (EC) method, the aerodynamic gradient (AG) method, and the relaxed eddy accumulation (REA) method. Although the EC method has been widely adopted in measuring soil-atmosphere exchange fluxes of nitrogen gases (N_2O, NO, etc.) (Soussana et al., 2007; Stella et al., 2012), it is difficult to be applied in HONO flux measurement due to the lack of highly sensitive and fast HONO measurement techniques (Von Der Heyden et al., 2022; Xue et al., 2019a). The AG and REA methods have been developed and applied to HONO flux measurements in recent years, providing a good option to measure HONO flux. However, available flux measurements are still limited and most of them were conducted over a short period of normally less than one month. Long-period measurements are still lacking (Laufs et al., 2017; Sörgel et al., 2015; Von Der Heyden et al., 2022; Zhou et al., 2011). Chamber methods, including static chamber and dynamic chamber, were usually used in studying emission factors of nitrogen gases (EF, the ratio of nitrogen emission to application). The static chamber method cannot be used to measure water-soluble gases (HONO, NH_3, etc.) because of the potential formation of water film on the inner surface of the chamber due to soil water evaporation (Xue et al., 2019a). The dynamic chamber method uses ambient air to flush the chamber to avoid the formation of water film, allowing the determination of HONO exchange fluxes between soil and atmosphere (Tang et al., 2019; Xue et al., 2019a). Particularly, the dynamic chamber method holds the advantage (low cost, etc.) to be implemented with several parallel experiments compared to others. For instance, HONO fluxes from soils with different treatments (i.e., different fertilizer application rates) can be easily achieved by building several chamber systems. A

https://doi.org/10.5194/egusphere-2023-1223
Preprint. Discussion started: 10 July 2023

systematic and long-term measurement of soil HONO flux is lacking, resulting in limitations in estimating the HONO emission factor (EF_{HONO}) (Xue et al., 2022a). It thereby also limits the understanding of the reactive nitrogen budget at an annual scale. With the reduction in reactive nitrogen emissions from anthropogenic combustion processes, natural emissions, including emissions from agricultural fields, are becoming more and more important. About one-third of the world's nitrogen fertilizer is consumed in China, indicating a strong potential for reactive nitrogen emissions. Moreover, with the agricultural intensification, more and more farmland implemented mechanization operations, leading to changes in fertilizer application methods. Currently, two fertilizer application methods are used in China: deep fertilization (DF) during machine sowing and spreading fertilizer (SF) on the soil surface (Nkebiwe et al., 2016; Pan et al., 2017), and the former one is becoming popular used in recent years. Our recent study observed high soil HONO emissions under SF conditions (Xue et al., 2022a). Therefore, it is necessary to conduct measurements under DF conditions considering that the emissions may change as fertilizer application method.

In this study, soil-atmosphere HONO exchange fluxes were measured by an open-top dynamic chamber (OTDC) system during the whole growing season of summer maize in the North China Plain (NCP). HONO fluxes from soils with several treatments were determined in parallel, which enables the understanding of the influencing factors of HONO emissions and the discussion of potential emission reduction strategies, etc. In addition, for the first time, the cumulative emissions and emission factors of HONO from the agricultural soils were calculated based on our long-period flux measurements crossing a whole growing season, benefitting the estimation of yearly soil HONO emissions at a national scale assessment of their atmospheric impacts.

2 Methods

2.1 Study site

The field flux measurement was conducted at the Station of Rural Environmental, Research Center for Eco-Environmental Sciences (SRE-RCEES, 38°71′N, 115°15′E),

https://doi.org/10.5194/egusphere-2023-1223
Preprint. Discussion started: 10 July 2023

located in Wangdu County, Hebei Province, China. The station is surrounded by vast agricultural fields, with winter wheat and summer maize rotation. More detailed descriptions of the measurement site can be found in our previous studies (Song et al., 2022a; Song et al., 2022b).

During the summer maize season, two different treatments were designed in the experiment fields: CK (control, normal flood irrigation but no fertilization for decades) and NP (fertilizer deep placement and normal flood irrigation, same as local farmers). In the experimental fields, summer maize was sown on June 17, 2021, and harvested on September 27, 2021. Only one fertilizer application event was conducted during the maize season. A typical-used compound fertilizer (N: P_2O_5: K_2O = 28%: 6%: 6%) was mechanized and buried to a depth of 8–10 cm when sowing maize seeds. The fertilizer application rate of the NP treatments was 300 kg N ha^{-1}, which is the typical amount used by local farmers.

2.2 Flux measurements

HONO exchange fluxes were measured by an OTDC system, which is updated based on our previous design (Xue et al., 2019a) (I.D. of 32 cm, 80 cm in height). Eight chambers (six experiment chambers, Exp-chambers, and two reference chambers, Ref-chambers) were divided into two groups (NP and CK) to obtain HONO flux from soils with different treatments (see Section 2.1). As shown in Figure 1, each group contains three replicated Exp-chambers and one Ref-chamber that are flushed by the same air pumped from the top of the metal sample tube (I.D. of 4 cm, 2 m in height, with the inner wall coated with Teflon film). The layout and construction of the OTDC system and other equipment are shown in Figure 1. Note that both fluxes from the NP and CK plots include heterogeneous HONO formation on the ground surface, which leads to an overestimation of soil HONO flux (Xue et al., 2019a). Through the comparison between flux from the NP and CK groups, we can distinguish the relative importance of soil emissions and NO_2 heterogeneous reactions and determine the net effect of fertilizer use.

https://doi.org/10.5194/egusphere-2023-1223
Preprint. Discussion started: 10 July 2023

HONO was continuously sampled by stripping coils with the absorption solution of ultrapure water. The sampling interval was normally set at 12 h for all eight chambers during the whole measurement period. To obtain the diurnal profiles of HONO emissions, the sampling interval was reduced to 2 h for one experimental chamber and one reference chamber in the NP group during pre-fertilization and post-fertilization periods. All samples were timely analyzed by an ion chromatography system (IC6200, WAYEE, China) (Xue et al., 2019b).

The soil HONO exchange flux (F_{HONO}, ng N m^{-2} s^{-1}) can be obtained by the difference of HONO concentrations in the Exp-chambers and Ref-chamber (Xue et al., 2019a):

$$F_{HONO} = \frac{(HONO_{exp} - HONO_{ref}) \times F_{flush} \times M_N \times P}{R \times T \times S} \times \frac{1}{60} \qquad (eq-1)$$

Where $HONO_{exp}$, $HONO_{ref}$, F_{flush}, M_N, P, R, T, and S are the HONO concentrations (ppbv) in the Exp-chambers and Ref-chamber, the flushing flow (20 L min^{-1}), the molar mass of N (14 g mol^{-1}), the atmospheric pressure (kPa), the ideal gas constant (8.314 L kPa mol^{-1} k^{-1}), the atmospheric thermodynamic temperature (K), and the area of the soil covered by the chamber (m^{-2}), respectively.

The emission factor of HONO (EF_{HONO}, %) relative to the amount of applied nitrogen can be calculated based on the following formula:

$$EF_{HONO} = \frac{E_{NP} - E_{CK}}{TN} \times 100\% \qquad (eq-2)$$

where E_{NP} and E_{CK} are the amounts of the cumulative HONO-N emissions (kg N ha^{-1}) from the fertilized plots and the control plots, respectively. TN is the total N input in the NP treatment field (kg N ha^{-1}).

2.3 Measurements of meteorology and soil characteristics

Meteorological parameters, including temperature, relative humidity (RH), pressure, wind speed (WS), wind direction (WD), precipitation, and solar radiation (SR), were recorded by an auto weather station (Vaisala WXT520, Finland). The photolysis frequency of NO_2 ($J(NO_2)$) was measured by a 2-π $J(NO_2)$ filter radiometer (MetCon, Germany). However, $J(NO_2)$ was not measured during August 18–27. Instead, it was

https://doi.org/10.5194/egusphere-2023-1223
Preprint. Discussion started: 10 July 2023

estimated via a high correlation between SR and $J(NO_2)$ (Figure S1, $J(NO_2)$ = 8.16×10^{-6} m^2 W^{-1} s^{-1} × DR + 2.17×10^{-4} s^{-1}, R=0.92).

The moisture of topsoil (0–5 cm) was expressed as water-filled pore space (WFPS), which was calculated by dividing the volumetric water content by the total soil porosity. The volumetric water content was measured twice a day (9:00 and 21:00 LT) by a soil humidity sensor (Stevens Hydra Probe II, USA) when collecting HONO samples, and total soil porosity was calculated according to the relationship: soil porosity = (1 – soil bulk density / 2.65), assuming a particle density of 2.65 g cm^{-3} (Linn and Doran, 1984). The topsoil samples were taken once a week by a ring sampler (5 cm diameter × 5 cm height) and the topsoil bulk density was determined gravimetrically by oven drying at 105 °C for 12 h.

To analyze the soil NH_4^+-N and NO_3^--N concentrations, soil samples were collected every three days for both NP and CK fields. Each sample was collected in four points and homogeneously mixed. 20 g of the mixed soil was extracted with 100 ml of 1 mol L^{-1} KCl solution, shaken in a rotary shaker (140 r min^{-1}) for 1 h, and filtered into sampling bottles. Samples were stored frozen until analyzed by a colorimetric continuous flow analyzer (Seal Analytical AutoAnalyzer 3, USA).

2.4 Data analysis

Mean tests, variance tests, and correlation analysis about HONO flux and other parameters were performed using the statistical software SPSS Statistic 24 (SPSS Inc., Chicago, USA). Figures were created by graphing software Origin 2018 (Origin Lab Corporation, Northampton, MA, USA) and ArcGIS 10.5 (ESRI Inc., California, USA).

3 Results and discussion

3.1 The variation of key meteorological and soil parameters

The variations of key meteorology (air temperature, RH, pressure, rainfall, and $J(NO_2)$) and soil parameters (soil NH_4^+-N and NO_3^--N concentrations, WFPS) during the measurement period are shown in Figure 2 and Figure S2, respectively. During the whole maize growing season (from June to September), average air temperature, RH,

https://doi.org/10.5194/egusphere-2023-1223
Preprint. Discussion started: 10 July 2023

and $J(NO_2)$ were 24.8°C, 72.3%, and 1.76×10^{-3} s^{-1}, respectively. The accumulative rainfall was 514 mm during this period, which was significantly higher than that in previous years (195–302 mm in the summer maize season during 2008–2011) (Zhang et al., 2014). The measured soil WFPS ranged from 33% to 82% and quickly increased following irrigation or precipitation, with a mean value of 59.1%. In the NP plots, the soil NH_4^+-N and NO_3^--N concentrations increased significantly after the application of nitrogen fertilizer (with averages of 48.0 and 112 mg kg^{-1} within 20 days after fertilization), whereas they remained at much lower levels throughout the whole maize season in the CK plots (with averages of 4.63 and 4.45 mg kg^{-1}).

3.2 Characteristics of HONO flux

Figure 3 shows the time series of HONO fluxes at a 12h-interval (daytime: 9:00–21:00, nighttime: 21:00–9:00) from the NP and CK plots ($F_{HONO\text{-}NP}$ and $F_{HONO\text{-}CK}$, average of three in-parallel duplications) during the whole maize season of 2021. HONO emission after fertilization showed a distinctly diurnal variation, that is, it was significantly higher in the daytime than at night, which will be discussed in the next section. According to the fertilization event and the characteristics of HONO flux, the whole observation was divided into three periods: (1) Pre-fertilization period (PFP, before June 18); (2) High HONO emission period (HEP, from June 18 to July 10); (3) Low HONO emission period (LEP, after July 10).

During the PFP period, the average $F_{HONO\text{-}NP}$ and $F_{HONO\text{-}CK}$ were 0.54 ± 0.35 and -0.51 ± 0.13 ng N m^{-2} s^{-1} from the NP and CK plots, respectively (Table S1). The higher level of $F_{HONO\text{-}NP}$ than $F_{HONO\text{-}CK}$ might be ascribed to the residual effect of fertilizer in the NP plots considering that CK plots have not been fertilized for years. Fluxes from CK plots are similar to observations at other sites with no nitrogen fertilization application, such as grass (Von Der Heyden et al., 2022) or forest (Ramsay et al., 2018; Sörgel et al., 2015; Zhou et al., 2011) regions.

After fertilization, as shown in Figure 3, $F_{HONO\text{-}NP}$ gradually increased and peaked on the fifteenth day, with a flux of 372 ng m^{-2} s^{-1}. The measured $F_{HONO\text{-}NP}$ then trended

https://doi.org/10.5194/egusphere-2023-1223
Preprint. Discussion started: 10 July 2023

downward but still maintained at a high level of 100 ng m^{-2} s^{-1} within 3 weeks after fertilization. In contrast, $F_{HONO-CK}$ always fluctuated around zero. During HEP, the average $F_{HONO-CK}$ value was -0.36 ± 0.04 ng N m^{-2} s^{-1}, which is similar to the NFP period (Table S1). In comparison, the mean value of $F_{HONO-NP}$ during HEP was 97.7 ± 8.6 ng N m^{-2} s^{-1}, revealing the large potential of fertilized soils in HONO emissions.

During the whole maize growing season, negative values of $F_{HONO-CK}$ were frequently observed at night, accounting for 72.5% of the total investigated data. Numerous studies on HONO flux measurement from unfertilized fields also reported this phenomenon, which is ascribed to nocturnal HONO deposition (Laufs et al., 2017; Ren et al., 2011; Tang et al., 2020), indicating the complexity of the role of the ground surface in nocturnal HONO production and deposition (Ramsay et al., 2018; Vandenboer et al., 2013; Vandenboer et al., 2015; Von Der Heyden et al., 2022). Nevertheless, it is worth noting that the high water content but no fertilization for the CK plots may contribute to the negative fluxes.

3.3 Diurnal variations of $F_{HONO-NP}$

During the high HONO emission period (HEP), the sampling interval was set at 2 h for one experimental chamber and one reference chamber, and 12 h for the other two experimental chambers in parallel. The 2-h interval measurements can provide detailed information about the diurnal variation. Figure 4 shows the time series of $F_{HONO-NP}$ with an interval of 2 h, which shows similar levels and trends to 12h interval measurements Diurnal variations of $HONO_{exp}$, $HONO_{ref}$, and $F_{HONO-NP}$ from the NP plot during PFP and HEP are shown in Figure 5. During PFP, $F_{HONO-NP}$ exhibited a distinct diurnal variation (Figure 5A), with a maximum of 0.38 ng N m^{-2} s^{-1} at noon and a minimum of 0.07 ng N m^{-2} s^{-1} in the early morning (Figure 5A).

During HEP, $HONO_{exp}$ increased by 1–2 orders of magnitude in comparison to that during the PFP period. As shown in Figure 5B, the $F_{HONO-NP}$ during HEP also showed "bell-shaped" diurnal variations, but with a much higher peak of 152 ng N m^{-2} s^{-1} at noon and a minimum of 40 ng N m^{-2} s^{-1} in the early morning. Similar diurnal variation

https://doi.org/10.5194/egusphere-2023-1223
Preprint. Discussion started: 10 July 2023

trends of HONO flux have been reported in previous studies (Tang et al., 2019; Tang et al., 2020; Von Der Heyden et al., 2022; Xue et al., 2019a; Zhou et al., 2011), while some studies also found morning peaks of the diurnal HONO flux (Laufs et al., 2017; Ren et al., 2011). Laufs et al. (2017) and Ren et al. (2011) also conducted flux measurements in farmland and they found high correlations between HONO flux and the product of NO_2 concentrations and $J(NO_2)$ or solar radiation. Their findings suggest that photosensitized heterogeneous reactions of NO_2 on the soil surfaces may be the main sources of the observed HONO flux. Measurements in Laufs et al. (2017) and Ren et al. (2011) are conducted during the non-fertilization period or a long time after fertilization, and hence their fluxes are about 2 orders of magnitude lower than those in this study. Note that the NO_2 or other NO_y reactions are not the main drivers of the observed flux in this study because the flux from the CK plots (no fertilization, representative for NO_y-to-HONO conversion on the ground surface, see Method) are about 2 orders of magnitude lower than those from the NP plots.

3.4 Comparison with previous flux measurements

The observed HONO flux, measurement methods, and fertilizer application rates in previous field measurements are shown in Table 1. Except for previous measurements at this agricultural site (Tang et al., 2019; Xue et al., 2019a; Xue et al., 2022a), fluxes from all other measurements are much lower than that in this study, which is due to the difference in fertilizer application rates. In this study, the maximum HONO flux at 2h-interval was 372 ng N m^{-2} s^{-1}, which was in the range of the maximums of HONO flux in previous field measurements (up to1515 ng N m^{-2} s^{-1}) (Laufs et al., 2017; Meng et al., 2022; Ren et al., 2011; Sörgel et al., 2015; Tang et al., 2019; Tang et al., 2020; Xue et al., 2019a; Zhou et al., 2011). In three previous studies in the summer maize field at the SRE-RCEES station, the peaks occurred within one week after fertilization, but their levels were variable depending on the fertilizer application rate (Tang et al., 2019; Xue et al., 2019a; Xue et al., 2022a). However, the peak of HONO flux occurred approximately two weeks after fertilization during this campaign. As mentioned in

Section 2.1, fertilizers were buried to a depth of 8–10 cm in this study, while they were spread on the soil surface in previous studies (Tang et al., 2019; Xue et al., 2019a; Xue et al., 2022a). Therefore, the relatively late occurrence of the HONO flux peak is probably caused by the slow dissolution due to the deep placement of nitrogen fertilizer. In addition to the impact on the occurrence time of peak flux, fertilizer application methods also lead to differences in levels of HONO emission fluxes. Compared with our study of fertilizer deep placement, Xue et al. (2019a) observed a peak HONO emission of 1515 ng N m^{-2} s^{-1} under the SF method, which is 4 times the peak in this study (372 ng N m^{-2} s^{-1}), although the fertilizer rate is close (300 kg N ha^{-1} in this study and 330 kg N ha^{-1} in Xue et al. (2019a)). Our recent study found high non-linear correlations between maximum HONO flux (F_{max}) and fertilizer application rate (FAR), that is, F_{max}=4.7×exp(-FAR/57.3)+15.3 (R^2=0.998, SF method, 0-350 kg N ha^{-1}) (Xue et al., 2022a). With the FAR used in this study (300 kg N ha^{-1}), the predicted F_{max} is ~890 ng N m^{-2} s^{-1}, much higher than the observation, indicating that compared to the SF method, the DF method can reduce soil HONO emissions, possibly through minimizing the mineral nitrogen content in topsoil (Ke et al., 2018; Liu et al., 2015; Weber et al., 2015). Therefore, the DF method is expected to be able to help reduce reactive nitrogen emissions from agricultural activities but needs more future systematic assessments.

3.5 Possible influencing factors

3.5.1 Rainfall and soil moisture

Soil nitrite generally originates from nitrification and/or denitrification processes, followed by the acid–base combination of soil NO_2^- (aq) and H^+ (aq) and the release of HONO to the atmosphere through liquid-gas partitioning (Bao et al., 2022; Su et al., 2011). As reported by Bao et al. (2022), equilibrium HONO concentrations (HONO*) directly affect soil HONO emissions. Rainfalls dilute soil nitrite concentration and thus HONO* decreases, inhibiting HONO emissions. On the five rainy days (rainfall > 1 mm) during HEP (June 23 and 27, July 1, 3, and 7), the soil WFPS immediately increased after rainfalls and the observed soil HONO fluxes decrease sharply as expected (Figure S3). Apart from June 23, the daytime HONO fluxes on the second day decreased to ~70% of the flux on the previous day. This finding suggests that rainfall significantly reduces soil HONO emissions but a new equilibrium can be reached shortly after the rain, although the soil water content was still high (Bao et al., 2022; Wang et al., 2021; Wu et al., 2019).

3.5.2 Temperature, atmospheric humidity, and solar irradiance

Atmospheric temperature, humidity, and light may also affect HONO soil emissions, given that they have similar or opposite diurnal variations to soil HONO emissions (Figure 5). Atmospheric temperature varies with soil temperature and can represent the topsoil temperature. At high temperatures, the nitrification process is more active to produce NO_2^- (Tourna et al., 2008), surface water evaporates faster, and thus more HONO is released (Su et al., 2011). Therefore, higher temperatures could promote soil HONO emission, as reported by laboratory studies (Oswald et al., 2013; Xue et al., 2022a), which also helps to explain the observed diurnal profiles of HONO flux.

In this study, we find that the air temperature positively correlated with HONO fluxes during PFP (Figure 6A, R = 0.73) and HEP (Figure 6B, R = 0.93). In contrast, HONO fluxes behave oppositely with air RH, with high correlation coefficients of 0.74 and 0.93 during PFP and HEP, respectively (Figure 6C–D). Higher RH could inhibit the water evaporation of the topsoil and may also increase topsoil content, limiting the release of soil nitrite to the atmosphere in the form of HONO (Bao et al., 2022; Su et al., 2011; Weber et al., 2015; Xue et al., 2022a).

Additionally, solar radiation seems to be a factor that favors soil HONO emissions, given that a positive correlation (R > 0.8) was found between diurnal HONO flux and $J(NO_2)$ (Figures 6E–F). Before fertilization, soil HONO emissions may originate from light-related processes, such as the photosensitive heterogeneous reactions of NO_2 on the soil surfaces, the photolysis of nitrate on the soil surface, etc. (Laufs et al., 2017; Ren et al., 2011; Stemmler et al., 2006; Von Der Heyden et al., 2022; Zhou et al., 2011).

https://doi.org/10.5194/egusphere-2023-1223
Preprint. Discussion started: 10 July 2023

However, as discussed before, the observed fluxes after fertilization were mainly from microbial processes rather than surface NO_y-to-HONO reactions. Therefore, the strong correlations between $J(NO_2)$ and HONO flux may be because solar irradiance could warm and dry the topsoil (Tang et al., 2019). Hence, we suspect that solar radiation plays an indirect role in soil HONO emissions by affecting the temperature of the topsoil. This is also consistent with our previous laboratory experiments demonstrating no enhancement effect of radiation on soil HONO emissions (Xue et al., 2022a).

3.6 Atmospheric impacts and implications

3.6.1 Impact on daytime HONO budget

Strong daytime unknown HONO sources are commonly observed in the summer NCP, which may be related to soil emissions (Liu et al., 2019; Song et al., 2022a; Xue et al., 2021). Therefore, it is necessary to study whether the soil HONO emissions can explain the unknown source strengths. On average, the observed HONO flux was around 46–119 ng m^{-2} s^{-1} (Figure 5B) in the daytime during HEP. The flux can explain unknown HONO strength of 3–7.5 ppb h^{-1} when assuming a mixing layer height of 100 m (Song et al., 2022b; Su et al., 2011; Xue et al., 2022b), which could cover the reported unknown HONO source (1.6–4.3 ppb h^{-1}) in the agricultural regions (Liu et al., 2019; Su et al., 2008; Xue et al., 2021). Hence, the HONO emission from fertilized soil acts as an important and even dominant source to explain the missing daytime HONO source, suggesting the potential impact of soil HONO emissions on regional air pollution and revealing the necessity of implementing soil HONO emissions in regional chemistry-transport models.

3.6.2 Implication on regional reactive nitrogen budget

Flux measurements throughout the whole growing season allow the estimation of cumulative emissions and emission factors, which helps to study the impact of fertilizer-derived HONO emissions on the reactive nitrogen budget. This is becoming more and more important relative to the decreasing anthropogenic emissions decreasing in China. However, to the best of our knowledge, there is no report on HONO

https://doi.org/10.5194/egusphere-2023-1223
Preprint. Discussion started: 10 July 2023

cumulative emissions and emission factors from nitrogen fertilizer applied to agriculture fields. In this study, we obtained the cumulative HONO emissions from NP and CK plots during the whole growing season of summer maize of 1.95 ± 0.21 and -0.09 ± 0.03 kg N ha^{-1}, respectively, and the EF_{HONO} of 0.68 ± 0.07% relative to the total applied nitrogen. The obtained EF_{HONO} is even at a similar level to EF_{NO} (0.24–0.82%) and EF_{N2O} (1.1–3.8%) as observed from the maize fields at the same site (Tian et al., 2017a; Tian et al., 2017b; Zhang et al., 2014), indicating the non-negligible contribution of soil HONO emission in soil nitrogen loss (Wang et al., 2023).

On a national scale, although the total fertilizer application amount has shown a downward trend after 2015, the current fertilizer application amount is still higher than that in 1978 by a factor of 5 (Figure 8A). The national nitrogen and compound fertilizer application amounts were 18 and 22 Tg in 2020 (data source: the China Statistical Yearbooks, http://www.stats.gov.cn/tjsj/ndsj/, last access: February 27, 2023). Assuming nitrogen accounts for 25% of the compound fertilizer, the total applied nitrogen is 24 Tg N in 2020. With an EF_{HONO} of 0.68%, the national fertilizer-induced soil HONO emission is around 0.16 Tg N yr^{-1}. Considering that the NCP region consumes a large portion of fertilizer in China and suffers severe O_3 pollution, soil HONO emissions need to be a particular concern in this region. As shown in Figure 8B, the applied nitrogen and the corresponding soil HONO emissions were 8.6 and 0.06 Tg N in the NCP in 2020, respectively (Figure 8A). The soil HONO emission is more than 30% of the annual regional soil NO_X emissions in the NCP (0.18 ± 0.01 Tg N yr^{-1}) (Lu et al., 2021), indicating that fertilized soils are important sources of both HONO and NO_X, affecting regional air quality in the NCP. It may as well indicate that soil HONO emissions should be considered in environmental policies, in terms of mitigating regional air pollution.

3.6.3 Implication on regional O_3 pollution

HONO emitted from fertilized soil can enhance regional oxidation capacity, leading to O_3 formation. For instance, Xue et al. (2021) conducted field measurements before and

https://doi.org/10.5194/egusphere-2023-1223
Preprint. Discussion started: 10 July 2023

after fertilization periods and found that the average daytime O_3 concentration increased from 50 ppbv during the no-fertilization period to 70 ppbv during the intensive fertilization period. Wu et al. (2022) estimated regional soil HONO emissions enhanced daytime OH concentrations by 10–60% and daytime O_3 concentrations by 0.5–1.5 ppb in Shanghai, China. Moreover, Wang et al. (2021) conducted model simulations with consideration of laboratory-derived soil HONO emissions and found that soil HONO emissions enhance the daytime OH concentration by 41%, and O_3 by 8% in the NCP. In this study, our long-period measurements cover the non-fertilization and fertilization periods, which allows an estimation of the impact of soil HONO emissions on atmospheric composition such as O_3 pollution. To do that, we use "O_3+NO_2" to represent the total oxidant concentrations (O_X) (Tang et al., 2009). Figures S4 and 7 show the time series and diurnal variation of O_3, NO_2, and O_X concentrations during PFP, HEP, and LEP, respectively. Compared with the PFP and LEP, the O_3 and NO_2 concentrations were higher during HEP by factors of 1.35–1.67 and 1.17–1.51, respectively. The averaged O_X concentrations were 68.4 ± 29.5 ppbv during HEP, which was 16.5 ppbv (31.8%) and 26.7 ppbv (64.1%) higher than those during PFP and LEP, respectively. The results demonstrate that fertilization can significantly affect regional O_3 formation in the NCP. Considering that the NCP region is a hot spot of O_3 pollution in recent years (Ma et al., 2021; Wang et al., 2017; Wang et al., 2020), the impacts of fertilizer-derived HONO emissions should be considered in terms of diagnosing O_3 pollution.

Therefore, although nitrogen fertilizer use is necessary to enhance crop yield, it can result in reactive nitrogen emissions that may cause environmental problems such as O_3 pollution. To address this issue, it is recommended to apply an appropriate fertilizer application rate that can optimize crop yields while minimizing reactive nitrogen emissions. In this study, field flux measurements reveal that the DF method can reduce soil HONO emissions compared to the SF method, which could be considered for future environmental policies. Moreover, nitrification inhibitors that are used to slow the

https://doi.org/10.5194/egusphere-2023-1223
Preprint. Discussion started: 10 July 2023

nitrification process (NH_{4+}→NO_2^-→NO_3^-) may also be able to reduce HONO emissions by reducing soil nitrite production. However, this needs more laboratory experiments to quantify the emission reduction efficiency as well as side effects. In the future, comparative field experiments, as well as laboratory experiments that utilize different fertilization methods, different fertilizer application rates, etc., should be conducted simultaneously to provide additional references for policymakers.

4 Conclusion

This study presents long-period measurements of HONO fluxes above agricultural fields in the North China Plain. Experiments are conducted simultaneously under two scenarios: normal fertilizer use (same as local farmers) and no fertilizer use, with three duplicated experiments conducted in parallel for each. The influencing factors and atmospheric implications of soil HONO emission were also discussed based on flux measurements in this and previous studies. The main conclusions are summarized as follows:

1) $F_{HONO-NP}$ and $F_{HONO-CK}$ show similar levels before fertilization, with negative values during nighttime, indicating that soil may occasionally act as a HONO sink at night. $F_{HONO-NP}$ can be largely enhanced by nitrogen fertilizer use as its average increases to 97.7 ± 8.6 ng N m^{-2} s^{-1} after fertilization. The observed $F_{HONO-NP}$ always show a bell-shaped diurnal variation, which is positively correlated to air temperature but opposite to relative humidity, implying their potential impacts on soil HONO emissions. Moreover, we find that HONO fluxes decline by 29.7–35.6% after rainfall due to significant increases in soil water content.
2) Soil is an important and even dominant source of daytime HONO. The observed HONO flux after fertilization can explain daytime HONO missing sources previously reported at this site and in other rural regions. Therefore, the synchronous measurements of fluxes and ambient concentrations are crucial to understanding the HONO budget as well as the follow-up atmospheric impacts on air quality, e.g., the regional abundance of O_3 and aerosol. Moreover, we found that

deep-burying fertilizer can reduce soil HONO emissions compared to traditional spreading on the soil surface, constituting a HONO emission reduction strategy.

3) Thanks to the long-period measurement covering the whole crop growing season, for the first time, we estimated a HONO emission factor of 0.68 ± 0.07% related to the applied nitrogen. The emission factor is even comparable to that of NO and N_2O, suggesting a non-negligible role of nitrogen loss through HONO emission. Accordingly, the fertilizer-induced cumulative HONO emissions are estimated to be 0.06 and 0.16 Tg N yr^{-1} from agriculture fields in the NCP and in China, respectively. Considering that nitrogen fertilizers are commonly used for agricultural fields and vegetable growing areas, this study also demonstrates the need for subsequent measurements of HONO fluxes on various underlying surfaces to provide an accurate estimation of reactive nitrogen (HONO, NO_X, etc.) emissions from those ecosystems.

In all, we demonstrate that soil HONO emissions and the promotion effect of fertilizer use should be considered in regional chemistry-transport models. It helps to improve the prediction of air quality, advance the understanding of the reactive nitrogen budget, and may as well benefit future environmental policies, in terms of mitigating regional air pollution.

Data availability. All the data used in this study are available at https://doi.org/10.5281/zenodo.8115973 (Song et al. 2023) and upon request from the corresponding authors.

Author contributions. YZ and YM designed the experiments. YS carried out the experiments. YS and CX led the data analysis and manuscript writing with inputs from all co-authors. CX, YZ, PL, FB, XL, and YM revised the manuscript.

Competing interests. The contact authors declare that neither they nor their co-authors have any competing interests.

https://doi.org/10.5194/egusphere-2023-1223
Preprint. Discussion started: 10 July 2023

Acknowledgments. The authors thank Liwei Guan for his help during the field experiments.

Financial support. This study was supported by the National Natural Science Foundation of China (No. 41931287, 42130714, 91544211, 41727805, 41975164, 41905109, and 21976108).

References

Bao, F., Cheng, Y., Kuhn, U., Li, G., Wang, W., Kratz, A. M., Weber, J., Weber, B., Poschl, U., and Su, H.: Key Role of Equilibrium HONO Concentration over Soil in Quantifying Soil-Atmosphere HONO Fluxes, Environ. Sci. Technol., 56, 2204-2212, https://doi.org/10.1021/acs.est.1c06716, 2022.

George, C., Strekowski, R. S., Kleffmann, J., Stemmler, K., and Ammann, M.: Photoenhanced uptake of gaseous NO_2 on solid organic compounds: a photochemical source of HONO?, Faraday Discuss., 130, 195-210, https://doi.org/10.1039/b417888m, 2005.

Han, C., Yang, W., Wu, Q., Yang, H., and Xue, X.: Heterogeneous Photochemical Conversion of NO_2 to HONO on the Humic Acid Surface under Simulated Sunlight, Environ. Sci. Technol., 50, 5017-5023, https://doi.org/10.1021/acs.est.5b05101, 2016.

Jia, C., Tong, S., Zhang, W., Zhang, X., Li, W., Wang, Z., Wang, L., Liu, Z., Hu, B., Zhao, P., and Ge, M.: Pollution characteristics and potential sources of nitrous acid (HONO) in early autumn 2018 of Beijing, Sci. Total Environ., 735, 139317, https://doi.org/10.1016/j.scitotenv.2020.139317, 2020.

Ke, J., He, R., Hou, P., Ding, C., Ding, Y., Wang, S., Liu, Z., Tang, S., Ding, C., Chen, L., and Li, G.: Combined controlled-released nitrogen fertilizers and deep placement effects of N leaching, rice yield and N recovery in machine-transplanted rice, Agr. Ecosyst. Environ., 265, 402-412, https://doi.org/10.1016/j.agee.2018.06.023, 2018.

https://doi.org/10.5194/egusphere-2023-1223
Preprint. Discussion started: 10 July 2023

Kim, S., VandenBoer, T. C., Young, C. J., Riedel, T. P., Thornton, J. A., Swarthout, B., Sive, B., Lerner, B., Gilman, J. B., Warneke, C., Roberts, J. M., Guenther, A., Wagner, N. L., Dube, W. P., Williams, E., and Brown, S. S.: The primary and recycling sources of OH during the NACHTT-2011 campaign: HONO as an important OH primary source in the wintertime, J. Geophys. Res.-Atmos., 119, 6886-6896, https://doi.org/10.1002/2013jd019784, 2014.

Kleffmann, J., Kurtenbach, R., Lorzer, J., Wiesen, P., Kalthoff, N., Vogel, B., and Vogel, H.: Measured and simulated vertical profiles of nitrous acid - Part I: Field measurements, Atmos. Environ., 37, 2949-2955, https://doi.org/10.1016/s1352-2310(03)00242-5, 2003.

Laufs, S., Cazaunau, M., Stella, P., Kurtenbach, R., Cellier, P., Mellouki, A., Loubet, B., and Kleffmann, J.: Diurnal fluxes of HONO above a crop rotation, Atmos. Chem. Phys., 17, 6907-6923, https://doi.org/10.5194/acp-17-6907-2017, 2017.

Li, D. D., Xue, L. K., Wen, L., Wang, X. F., Chen, T. S., Mellouki, A., Chen, J. M., and Wang, W. X.: Characteristics and sources of nitrous acid in an urban atmosphere of northern China: Results from 1-yr continuous observations, Atmos. Environ., 182, 296-306, https://doi.org/10.1016/j.atmosenv.2018.03.033, 2018.

Li, X., Brauers, T., Haseler, R., Bohn, B., Fuchs, H., Hofzumahaus, A., Holland, F., Lou, S., Lu, K. D., Rohrer, F., Hu, M., Zeng, L. M., Zhang, Y. H., Garland, R. M., Su, H., Nowak, A., Wiedensohler, A., Takegawa, N., Shao, M., and Wahner, A.: Exploring the atmospheric chemistry of nitrous acid (HONO) at a rural site in Southern China, Atmos. Chem. Phys., 12, 1497-1513, https://doi.org/10.5194/acp-12-1497-2012, 2012.

Li, X., Rohrer, F., Hofzumahaus, A., Brauers, T., Haeseler, R., Bohn, B., Broch, S., Fuchs, H., Gomm, S., Holland, F., Jaeger, J., Kaiser, J., Keutsch, F. N., Lohse, I., Lu, K., Tillmann, R., Wegener, R., Wolfe, G. M., Mentel, T. F., Kiendler-Scharr, A., and Wahner, A.: Missing Gas-Phase Source of HONO Inferred from Zeppelin

Measurements in the Troposphere, Science, 344, 292-296, https://doi.org/10.1126/science.1248999, 2014.

Linn, D. M. and Doran, J. W.: Effect of Water-Filled Pore Space on Carbon Dioxide and Nitrous Oxide Production in Tilled and Nontilled Soils, Soil Sci. Soc. Am. J., 48, 1267-1272, https://doi.org/10.2136/sssaj1984.03615995004800060013x, 1984.

Liu, T. Q., Fan, D. J., Zhang, X. X., Chen, J., Li, C. F., and Cao, C. G.: Deep placement of nitrogen fertilizers reduces ammonia volatilization and increases nitrogen utilization efficiency in no-tillage paddy fields in central China, Field Crop. Res., 184, 80-90, https://doi.org/10.1016/j.fcr.2015.09.011, 2015.

Liu, Y., Lu, K., Li, X., Dong, H., Tan, Z., Wang, H., Zou, Q., Wu, Y., Zeng, L., Hu, M., Min, K. E., Kecorius, S., Wiedensohler, A., and Zhang, Y.: A Comprehensive Model Test of the HONO Sources Constrained to Field Measurements at Rural North China Plain, Environ. Sci. Technol., 53, 3517-3525, https://doi.org/10.1021/acs.est.8b06367, 2019.

Lu, X., Ye, X., Zhou, M., Zhao, Y., Weng, H., Kong, H., Li, K., Gao, M., Zheng, B., Lin, J., Zhou, F., Zhang, Q., Wu, D., Zhang, L., and Zhang, Y.: The underappreciated role of agricultural soil nitrogen oxide emissions in ozone pollution regulation in North China, Nat. Commun., 12, 5021, https://doi.org/10.1038/s41467-021-25147-9, 2021.

Ma, X., Huang, J., Zhao, T., Liu, C., Zhao, K., Xing, J., and Xiao, W.: Rapid increase in summer surface ozone over the North China Plain during 2013–2019: a side effect of particulate matter reduction control?, Atmos. Chem. Phys., 21, 1-16, https://doi.org/10.5194/acp-21-1-2021, 2021.

Meng, F., Qin, M., Fang, W., Duan, J., Tang, K., Zhang, H., Shao, D., Liao, Z., Feng, Y., Huang, Y., Ni, T., Xie, P., Liu, J., and Liu, W.: Measurement of HONO flux using the aerodynamic gradient method over an agricultural field in the Huaihe River Basin, China, J. Environ. Sci., 114, 297-307, https://doi.org/10.1016/j.jes.2021.09.005, 2022.

https://doi.org/10.5194/egusphere-2023-1223
Preprint. Discussion started: 10 July 2023

Nkebiwe, P. M., Weinmann, M., Bar-Tal, A., and Müller, T.: Fertilizer placement to improve crop nutrient acquisition and yield: A review and meta-analysis, Field Crop. Res., 196, 389-401, https://doi.org/10.1016/j.fcr.2016.07.018, 2016.

Oswald, R., Behrendt, T., Ermel, M., Wu, D., Su, H., Cheng, Y., Breuninger, C., Moravek, A., Mougin, E., Delon, C., Loubet, B., Pommerening-Roeser, A., Soergel, M., Poeschl, U., Hoffmann, T., Andreae, M. O., Meixner, F. X., and Trebs, I.: HONO Emissions from Soil Bacteria as a Major Source of Atmospheric Reactive Nitrogen, Science, 341, 1233-1235, https://doi.org/10.1126/science.1242266, 2013.

Pan, S., Wen, X., Wang, Z., Ashraf, U., Tian, H., Duan, M., Mo, Z., Fan, P., and Tang, X.: Benefits of mechanized deep placement of nitrogen fertilizer in direct-seeded rice in South China, Field Crop. Res., 203, 139-149, https://doi.org/10.1016/j.fcr.2016.12.011, 2017.

Ramsay, R., Di Marco, C. F., Heal, M. R., Twigg, M. M., Cowan, N., Jones, M. R., Leeson, S. R., Bloss, W. J., Kramer, L. J., Crilley, L., Sörgel, M., Andreae, M., and Nemitz, E.: Surface–atmosphere exchange of inorganic water-soluble gases and associated ions in bulk aerosol above agricultural grassland pre- and postfertilisation, Atmos. Chem. Phys., 18, 16953-16978, https://doi.org/10.5194/acp-18-16953-2018, 2018.

Ren, X., Sanders, J. E., Rajendran, A., Weber, R. J., Goldstein, A. H., Pusede, S. E., Browne, E. C., Min, K. E., and Cohen, R. C.: A relaxed eddy accumulation system for measuring vertical fluxes of nitrous acid, Atmos. Meas. Tech., 4, 2093-2103, https://doi.org/10.5194/amt-4-2093-2011, 2011.

Seinfeld, J. H. and Pandis, S. N.: Atmospheric Chemistry and Physics: From Air Pollution to Climate Change, John Wiley & Sons, Hoboken, NJ, Wiley2016.

Song, Y., Zhang, Y., Liu, J., Zhang, C., Liu, C., Liu, P., and Mu, Y.: Rural vehicle emission as an important driver for the variations of summertime tropospheric ozone in the Beijing-Tianjin-Hebei region during 2014-2019, J. Environ. Sci., 114, 126-135, https://doi.org/10.1016/j.jes.2021.08.015, 2022a.

https://doi.org/10.5194/egusphere-2023-1223
Preprint. Discussion started: 10 July 2023

Song, Y., Zhang, Y., Xue, C., Liu, P., He, X., Li, X., and Mu, Y.: The seasonal variations and potential sources of nitrous acid (HONO) in the rural North China Plain, Environ. Pollut., 311, 119967, https://doi.org/10.1016/j.envpol.2022.119967, 2022b.

Song, Y., Xue, C., Zhang, Y., and Mu, Y.: Measurement Report: Exchange Fluxes of HONO over Agricultural Fields in the North China Plain [Data set]. Zenodo. https://doi.org/10.5281/zenodo.8115973, 2023.

Sörgel, M., Trebs, I., Wu, D., and Held, A.: A comparison of measured HONO uptake and release with calculated source strengths in a heterogeneous forest environment, Atmos. Chem. Phys., 15, 9237-9251, https://doi.org/10.5194/acp-15-9237-2015, 2015.

Soussana, J. F., Allard, V., Pilegaard, K., Ambus, P., Amman, C., Campbell, C., Ceschia, E., Clifton-Brown, J., Czobel, S., Domingues, R., Flechard, C., Fuhrer, J., Hensen, A., Horvath, L., Jones, M., Kasper, G., Martin, C., Nagy, Z., Neftel, A., Raschi, A., Baronti, S., Rees, R. M., Skiba, U., Stefani, P., Manca, G., Sutton, M., Tubaf, Z., and Valentini, R.: Full accounting of the greenhouse gas (CO_2, N_2O, CH_4) budget of nine European grassland sites, Agr. Ecosyst. Environ., 121, 121-134, https://doi.org/10.1016/j.agee.2006.12.022, 2007.

Spataro, F., Ianniello, A., Esposito, G., Allegrini, I., Zhu, T., and Hu, M.: Occurrence of atmospheric nitrous acid in the urban area of Beijing (China), Sci. Total Environ., 447, 210-224, https://doi.org/10.1016/j.scitotenv.2012.12.065, 2013.

Stella, P., Loubet, B., Laville, P., Lamaud, E., Cazaunau, M., Laufs, S., Bernard, F., Grosselin, B., Mascher, N., Kurtenbach, R., Mellouki, A., Kleffmann, J., and Cellier, P.: Comparison of methods for the determination of NO-O_3-NO_2 fluxes and chemical interactions over a bare soil, Atmos. Meas. Tech., 5, 1241-1257, https://doi.org/10.5194/amt-5-1241-2012, 2012.

Stemmler, K., Ammann, M., Donders, C., Kleffmann, J., and George, C.: Photosensitized reduction of nitrogen dioxide on humic acid as a source of nitrous acid, Nature, 440, 195-198, https://doi.org/10.1038/nature04603, 2006.

Stemmler, K., Ndour, M., Elshorbany, Y., Kleffmann, J., D'Anna, B., George, C., Bohn, B., and Ammann, M.: Light induced conversion of nitrogen dioxide into nitrous acid on submicron humic acid aerosol, Atmos. Chem. Phys., 7, 4237-4248, https://doi.org/10.5194/acp-7-4237-2007, 2007.

Su, H., Cheng, Y. F., Shao, M., Gao, D. F., Yu, Z. Y., Zeng, L. M., Slanina, J., Zhang, Y. H., and Wiedensohler, A.: Nitrous acid (HONO) and its daytime sources at a rural site during the 2004 PRIDE-PRD experiment in China, J. Geophys. Res.-Atmos., 113, D14312, https://doi.org/10.1029/2007jd009060, 2008.

Su, H., Cheng, Y., Oswald, R., Behrendt, T., Trebs, I., Meixner, F. X., Andreae, M. O., Cheng, P., Zhang, Y., and Poeschl, U.: Soil Nitrite as a Source of Atmospheric HONO and OH Radicals, Science, 333, 1616-1618, https://doi.org/10.1126/science.1207687, 2011.

Tan, Z. F., Fuchs, H., Lu, K. D., Hofzumahaus, A., Bohn, B., Broch, S., Dong, H. B., Gomm, S., Haseler, R., He, L. Y., Holland, F., Li, X., Liu, Y., Lu, S. H., Rohrer, F., Shao, M., Wang, B. L., Wang, M., Wu, Y. S., Zeng, L. M., Zhang, Y. S., Wahner, A., and Zhang, Y. H.: Radical chemistry at a rural site (Wangdu) in the North China Plain: observation and model calculations of OH, HO_2 and RO_2 radicals, Atmos. Chem. Phys., 17, 663-690, https://doi.org/10.5194/acp-17-663-2017, 2017.

Tan, Z. F., Rohrer, F., Lu, K. D., Ma, X. F., Bohn, B., Broch, S., Dong, H. B., Fuchs, H., Gkatzelis, G. I., Hofzumahaus, A., Holland, F., Li, X., Liu, Y., Liu, Y. H., Novelli, A., Shao, M., Wang, H. C., Wu, Y. S., Zeng, L. M., Hu, M., Kiendler-Scharr, A., Wahner, A., and Zhang, Y. H.: Wintertime photochemistry in Beijing: observations of ROx radical concentrations in the North China Plain during the BEST-ONE campaign, Atmos. Chem. Phys., 18, 12391-12411, https://doi.org/10.5194/acp-18-12391-2018, 2018.

https://doi.org/10.5194/egusphere-2023-1223
Preprint. Discussion started: 10 July 2023

Tang, G., Li, X., Wang, Y., Xin, J., and Ren, X.: Surface ozone trend details and interpretations in Beijing, 2001-2006, Atmos. Chem. Phys., 9, 8813-8823, https://doi.org/10.5194/acp-9-8813-2009, 2009.

Tang, K., Qin, M., Duan, J., Fang, W., Meng, F. H., Liang, S. X., Xie, P. H., Liu, J. G., Liu, W. Q., Xue, C. Y., and Mu, Y. J.: A dual dynamic chamber system based on IBBCEAS for measuring fluxes of nitrous acid in agricultural fields in the North China Plain, Atmos. Environ., 196, 10-19, https://doi.org/10.1016/j.atmosenv.2018.09.059, 2019.

Tang, K., Qin, M., Fang, W., Duan, J., Meng, F., Ye, K., Zhang, H., Xie, P., Liu, J., Liu, W., Feng, Y., Huang, Y., and Ni, T.: An automated dynamic chamber system for exchange flux measurement of reactive nitrogen oxides (HONO and NO_X) in farmland ecosystems of the Huaihe River Basin, China, Sci. Total Environ., 745, 140867, https://doi.org/10.1016/j.scitotenv.2020.140867, 2020.

Tian, D., Zhang, Y., Mu, Y., Zhou, Y., Zhang, C., and Liu, J.: The effect of drip irrigation and drip fertigation on N_2O and NO emissions, water saving and grain yields in a maize field in the North China Plain, Sci. Total Environ., 575, 1034-1040, https://doi.org/10.1016/j.scitotenv.2016.09.166, 2017a.

Tian, D., Zhang, Y., Zhou, Y., Mu, Y., Liu, J., Zhang, C., and Liu, P.: Effect of nitrification inhibitors on mitigating N_2O and NO emissions from an agricultural field under drip fertigation in the North China Plain, Sci. Total Environ., 598, 87-96, https://doi.org/10.1016/j.scitotenv.2017.03.220, 2017b.

Tourna, M., Freitag, T. E., Nicol, G. W., and Prosser, J. I.: Growth, activity and temperature responses of ammonia-oxidizing archaea and bacteria in soil microcosms, Environ. Microbiol., 10, 1357-1364, https://doi.org/10.1111/j.1462-2920.2007.01563.x, 2008.

VandenBoer, T. C., Young, C. J., Talukdar, R. K., Markovic, M. Z., Brown, S. S., Roberts, J. M., and Murphy, J. G.: Nocturnal loss and daytime source of nitrous acid through reactive uptake and displacement, Nat. Geosci., 8, 55-60, https://doi.org/10.1038/Ngeo2298, 2015.

VandenBoer, T. C., Brown, S. S., Murphy, J. G., Keene, W. C., Young, C. J., Pszenny, A. A. P., Kim, S., Warneke, C., de Gouw, J. A., Maben, J. R., Wagner, N. L., Riedel, T. P., Thornton, J. A., Wolfe, D. E., Dube, W. P., Ozturk, F., Brock, C. A., Grossberg, N., Lefer, B., Lerner, B., Middlebrook, A. M., and Roberts, J. M.: Understanding the role of the ground surface in HONO vertical structure: High resolution vertical profiles during NACHTT-11, J. Geophys. Res.-Atmos., 118, 10155-10171, https://doi.org/10.1002/jgrd.50721, 2013.

von der Heyden, L., Wißdorf, W., Kurtenbach, R., and Kleffmann, J.: A relaxed eddy accumulation (REA) LOPAP system for flux measurements of nitrous acid (HONO), Atmos. Meas. Tech., 15, 1983-2000, https://doi.org/10.5194/amt-15-1983-2022, 2022.

Wang, T., Xue, L., Brimblecombe, P., Lam, Y. F., Li, L., and Zhang, L.: Ozone pollution in China: A review of concentrations, meteorological influences, chemical precursors, and effects, Sci. Total Environ., 575, 1582-1596, https://doi.org/10.1016/j.scitotenv.2016.10.081, 2017.

Wang, Y., Fu, X., Wang, T., Ma, J., Gao, H., Wang, X., and Pu, W.: Large Contribution of Nitrous Acid to Soil-Emitted Reactive Oxidized Nitrogen and Its Effect on Air Quality, Environ. Sci. Technol., https://doi.org/10.1021/acs.est.2c07793, 2023.

Wang, Y., Fu, X., Wu, D., Wang, M., Lu, K., Mu, Y., Liu, Z., Zhang, Y., and Wang, T.: Agricultural Fertilization Aggravates Air Pollution by Stimulating Soil Nitrous Acid Emissions at High Soil Moisture, Environ. Sci. Technol., 55, 14556-14566, https://doi.org/10.1021/acs.est.1c04134, 2021.

Wang, Y. H., Gao, W. K., Wang, S., Song, T., Gong, Z. Y., Ji, D. S., Wang, L. L., Liu, Z. R., Tang, G. Q., Huo, Y. F., Tian, S. L., Li, J. Y., Li, M. G., Yang, Y., Chu, B. W., Petaja, T., Kerminen, V. M., He, H., Hao, J. M., Kulmala, M., Wang, Y. S., and Zhang, Y. H.: Contrasting trends of $PM_{2.5}$ and surface-ozone concentrations in

China from 2013 to 2017, Natl. Sci. Rev., 7, 1331-1339, https://doi.org/10.1093/nsr/nwaa032, 2020.

Weber, B., Wu, D., Tamm, A., Ruckteschler, N., Rodriguez-Caballero, E., Steinkamp, J., Meusel, H., Elbert, W., Behrendt, T., Sorgel, M., Cheng, Y., Crutzen, P. J., Su, H., and Poschl, U.: Biological soil crusts accelerate the nitrogen cycle through large NO and HONO emissions in drylands, Proc. Natl. Acad. Sci. USA, 112, 15384-15389, https://doi.org/10.1073/pnas.1515818112, 2015.

Wong, K. W., Tsai, C., Lefer, B., Haman, C., Grossberg, N., Brune, W. H., Ren, X., Luke, W., and Stutz, J.: Daytime HONO vertical gradients during SHARP 2009 in Houston, TX, Atmos. Chem. Phys., 12, 635-652, https://doi.org/10.5194/acp-12-635-2012, 2012.

Wu, D., Zhang, J., Wang, M., An, J., Wang, R., Haider, H., Xu ‐ Ri, Huang, Y., Zhang, Q., Zhou, F., Tian, H., Zhang, X., Deng, L., Pan, Y., Chen, X., Yu, Y., Hu, C., Wang, R., Song, Y., Gao, Z., Wang, Y., Hou, L., and Liu, M.: Global and Regional Patterns of Soil Nitrous Acid Emissions and Their Acceleration of Rural Photochemical Reactions, J. Geophys. Res.-Atmos., 127, https://doi.org/10.1029/2021jd036379, 2022.

Wu, D. M., Horn, M. A., Behrendt, T., Muller, S., Li, J. S., Cole, J. A., Xie, B., Ju, X., Li, G., Ermel, M., Oswald, R., Frohlich-Nowoisky, J., Hoor, P., Hu, C., Liu, M., Andreae, M. O., Poschl, U., Cheng, Y., Su, H., Trebs, I., Weber, B., and Sorgel, M.: Soil HONO emissions at high moisture content are driven by microbial nitrate reduction to nitrite: tackling the HONO puzzle, ISME J, 13, 1688-1699, https://doi.org/10.1038/s41396-019-0379-y, 2019.

Xue, C., Ye, C., Zhang, Y., Ma, Z., Liu, P., Zhang, C., Zhao, X., Liu, J., and Mu, Y.: Development and application of a twin open-top chambers method to measure soil HONO emission in the North China Plain, Sci. Total Environ., 659, 621-631, https://doi.org/10.1016/j.scitotenv.2018.12.245, 2019a.

Xue, C., Ye, C., Liu, P., Zhang, C., Su, H., Bao, F., Cheng, Y., Catoire, V., Ma, Z., Zhao, X., Lu, K., Liu, Y., McGillen, M., Mellouki, A., and Mu, Y.: Strong HONO Emissions from Fertilized Soil in the North China Plain Driven by Nitrification and Water Evaporation, PREPRINT (Version 3) available at Research Square, https://doi.org/10.21203/rs.3.rs-2045348/v3, 2022a.

Xue, C., Ye, C., Kleffmann, J., Zhang, W., He, X., Liu, P., Zhang, C., Zhao, X., Liu, C., Ma, Z., Liu, J., Wang, J., Lu, K., Catoire, V., Mellouki, A., and Mu, Y.: Atmospheric measurements at Mt. Tai – Part II: HONO budget and radical (RO_X + NO_3) chemistry in the lower boundary layer, Atmos. Chem. Phys., 22, 1035-1057, https://doi.org/10.5194/acp-22-1035-2022, 2022b.

Xue, C., Ye, C., Ma, Z., Liu, P., Zhang, Y., Zhang, C., Tang, K., Zhang, W., Zhao, X., Wang, Y., Song, M., Liu, J., Duan, J., Qin, M., Tong, S., Ge, M., and Mu, Y.: Development of stripping coil-ion chromatograph method and intercomparison with CEAS and LOPAP to measure atmospheric HONO, Sci. Total Environ., 646, 187-195, https://doi.org/10.1016/j.scitotenv.2018.07.244, 2019b.

Xue, C., Ye, C., Zhang, C., Catoire, V., Liu, P., Gu, R., Zhang, J., Ma, Z., Zhao, X., Zhang, W., Ren, Y., Krysztofiak, G., Tong, S., Xue, L., An, J., Ge, M., Mellouki, A., and Mu, Y.: Evidence for Strong HONO Emission from Fertilized Agricultural Fields and its Remarkable Impact on Regional O_3 Pollution in the Summer North China Plain, ACS Earth Space Chem., 5, 340-347, https://doi.org/10.1021/acsearthspacechem.0c00314, 2021.

Xue, C., Zhang, C., Ye, C., Liu, P., Catoire, V., Krysztofiak, G., Chen, H., Ren, Y., Zhao, X., Wang, J., Zhang, F., Zhang, C., Zhang, J., An, J., Wang, T., Chen, J., Kleffmann, J., Mellouki, A., and Mu, Y.: HONO Budget and Its Role in Nitrate Formation in the Rural North China Plain, Environ. Sci. Technol., 54, 11048-11057, https://doi.org/10.1021/acs.est.0c01832, 2020.

Zhang, J., Chen, J., Xue, C., Chen, H., Zhang, Q., Liu, X., Mu, Y., Guo, Y., Wang, D., Chen, Y., Li, J., Qu, Y., and An, J.: Impacts of six potential HONO sources on

https://doi.org/10.5194/egusphere-2023-1223
Preprint. Discussion started: 10 July 2023

HO(x) budgets and SOA formation during a wintertime heavy haze period in the North China Plain, Sci. Total Environ., 681, 110-123, https://doi.org/10.1016/j.scitotenv.2019.05.100, 2019.

Zhang, N., Zhou, X., Shepson, P. B., Gao, H., Alaghmand, M., and Stirm, B.: Aircraft measurement of HONO vertical profiles over a forested region, Geophys. Res. Lett., 36, n/a-n/a, https://doi.org/10.1029/2009gl038999, 2009.

Zhang, N., Zhou, X., Bertman, S., Tang, D., Alaghmand, M., Shepson, P. B., and Carroll, M. A.: Measurements of ambient HONO concentrations and vertical HONO flux above a northern Michigan forest canopy, Atmos. Chem. Phys., 12, 8285-8296, https://doi.org/10.5194/acp-12-8285-2012, 2012.

Zhang, Y., Mu, Y., Zhou, Y., Liu, J., and Zhang, C.: Nitrous oxide emissions from maize–wheat field during 4 successive years in the North China Plain, Biogeosciences, 11, 1717-1726, https://doi.org/10.5194/bg-11-1717-2014, 2014.

Zhou, X. L., Zhang, N., TerAvest, M., Tang, D., Hou, J., Bertman, S., Alaghmand, M., Shepson, P. B., Carroll, M. A., Griffith, S., Dusanter, S., and Stevens, P. S.: Nitric acid photolysis on forest canopy surface as a source for tropospheric nitrous acid, Nat. Geosci., 4, 440-443, https://doi.org/10.1038/Ngeo1164, 2011.

https://doi.org/10.5194/egusphere-2023-1223
Preprint. Discussion started: 10 July 2023

Tables

Table 1. Summary of the maximum values of HONO flux in field measurements over different soil types and corresponding measurement methods and fertilizer application rates in the world.

Soil type	Method	Maximum HONO flux (ng N m^{-2} s^{-1})	Fertilizer application rate (kg N ha^{-1})	References
Agriculture	REA[a]	7.0	0	1
Forest	REA	2.8	0	2
Forest	REA	18.3	0	3
Grassland	REA	2.3	0	4
Forest	AG[b]	0.98	0	5
Maize	AG	2.3[d]	33.4	6
Wheat	AG	15.4	69	7
Maize	OTDC[c]	1515	330	8
Maize	OTDC	40	180	9
Wheat	OTDC	7.69	69	10
Agriculture	OTDC	348	247	11
Maize	OTDC	372	300	This study

[a]: relaxed eddy accumulation; [b]: aerodynamic gradient; [c]: open-top dynamic chamber; [d]: maximum of the diurnal HONO fluxes.

1:(Ren et al., 2011); 2: (Zhou et al., 2011); 3: (Zhang et al., 2012); 4: (Von Der Heyden et al., 2022); 5: (Sörgel et al., 2015); 6: (Laufs et al., 2017); 7: (Meng et al., 2022); 8: (Xue et al., 2019a); 9: (Tang et al., 2019); 10: (Tang et al., 2020); 11:(Xue et al., 2022a).

https://doi.org/10.5194/egusphere-2023-1223
Preprint. Discussion started: 10 July 2023

Figures

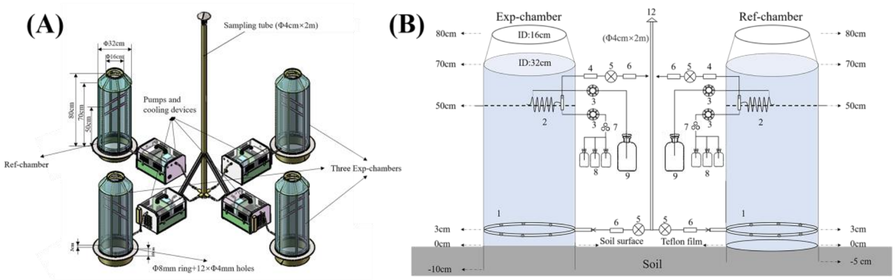

Figure 1. The layout (A) and constructions (B) of the OTDC system and other equipment (upgraded based on Xue et al. (2019a)). 1. Stainless collar. 2. Stripping coil. 3. Peristaltic pump. 4. Drying tube. 5. Air pump. 6. Flow regulator. 7. Valve of 24 accesses. 8. Sample bottle. 9. Absorption solution bottle. 10. Air mixing device. 11. Standard gases or synthesis air. 12. Sampling tube. Exp-chamber: experimental chamber; Ref-chamber: reference chamber.

https://doi.org/10.5194/egusphere-2023-1223
Preprint. Discussion started: 10 July 2023

805

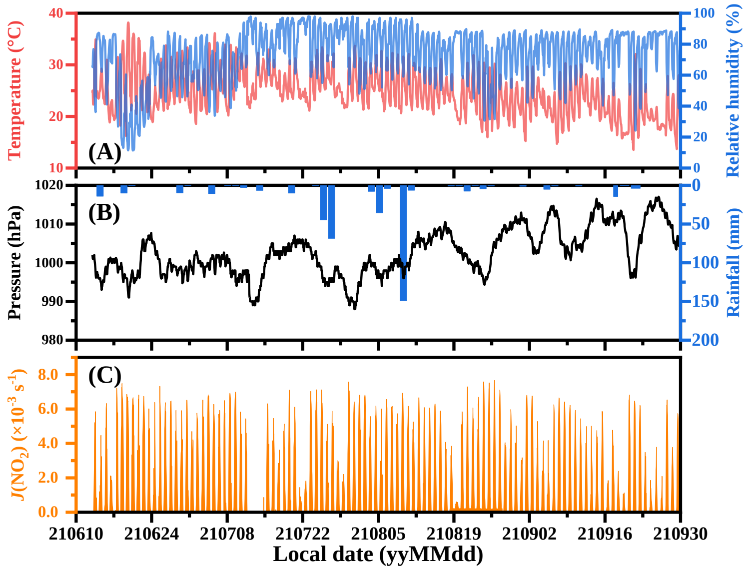

Figure 2. The time series of meteorology (A: air temperature and relative humidity; B: air pressure and rainfall; C: the photolysis frequency of NO_2 ($J(NO_2)$) during maize season at the experiment site.

https://doi.org/10.5194/egusphere-2023-1223
Preprint. Discussion started: 10 July 2023

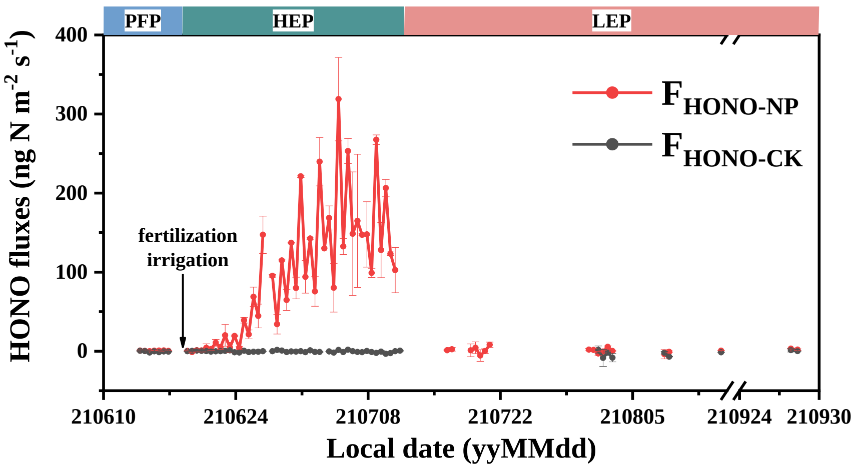

Figure 3. Variations of HONO fluxes at 12 h intervals from NP and CK plots ($F_{HONO-NP}$ and $F_{HONO-CK}$) during the maize season of 2021. PFP: pre-fertilization period, before June 18; HEP: high emission period, from June 18 to July 10; LEP: low emission period, after July 10). The error bars represent the standard deviations of HONO fluxes from NP or CK plots (n=3).

https://doi.org/10.5194/egusphere-2023-1223
Preprint. Discussion started: 10 July 2023

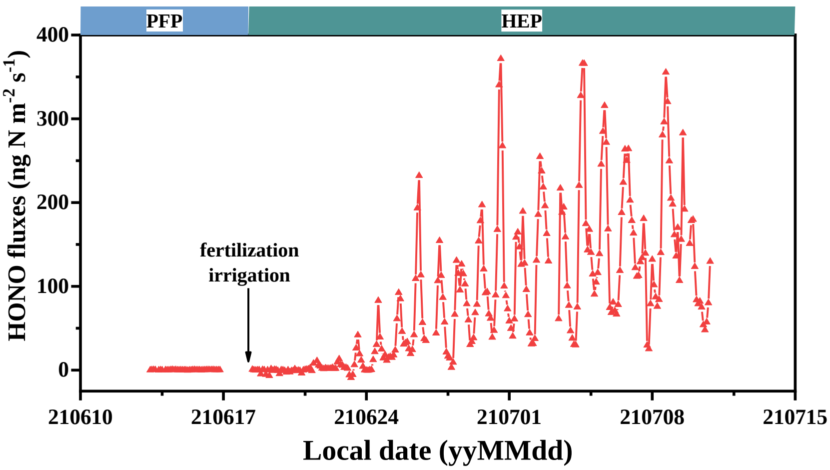

Figure 4. Variations of 2-h interval HONO fluxes from the NP plots from June 13 to July 10, 2021.

820

https://doi.org/10.5194/egusphere-2023-1223
Preprint. Discussion started: 10 July 2023

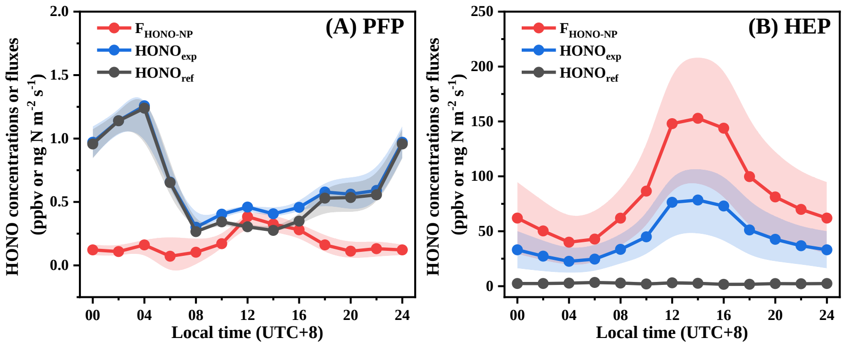

Figure 5. Diurnal variations of $HONO_{exp}$, $HONO_{ref}$, and HONO fluxes during PFP and HEP from the NP plot. Shadows represent half of the standard deviation (±0.5 σ).

https://doi.org/10.5194/egusphere-2023-1223
Preprint. Discussion started: 10 July 2023

825

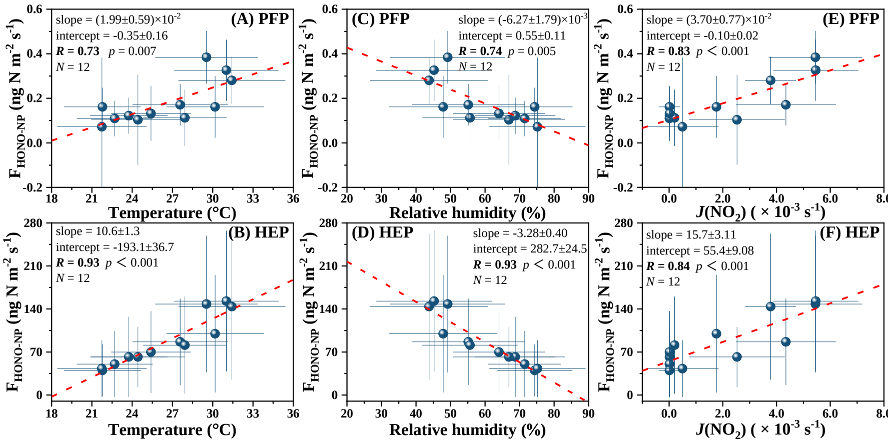

Figure 6. Correlation of the diurnal $F_{HONO\text{-}NP}$ with the meteorological parameters (air temperature, air relative humidity, ad $J(NO_2)$) during PFP and HEP.

https://doi.org/10.5194/egusphere-2023-1223
Preprint. Discussion started: 10 July 2023

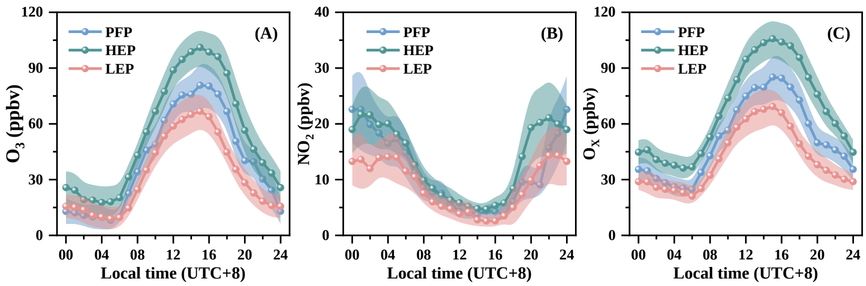

830 **Figure 7.** The diurnal variations of O_3, NO_2, and O_X (O_3 + NO_2) concentrations during PFP, HEP, and LFP. Shadows represent half of the standard deviation (±0.5 σ).

https://doi.org/10.5194/egusphere-2023-1223
Preprint. Discussion started: 10 July 2023

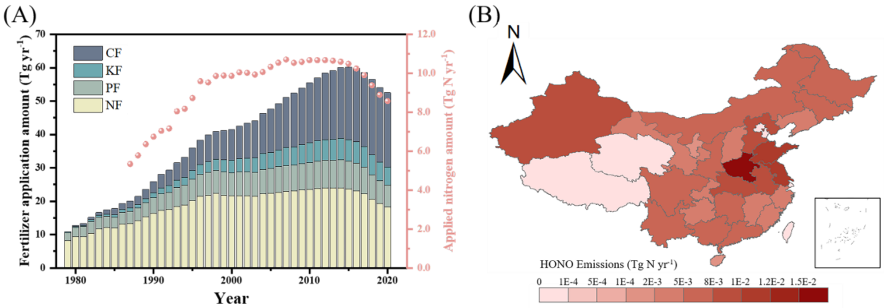

Figure 8. (A): the national fertilizer application amount (CF: compound fertilizer; KF:
835 potash fertilizer; PF: phosphatic fertilizer; NF: nitrogen fertilizer) in China during 1978–2020 and applied nitrogen amount (nitrogen fertilizer amount + 0.25 × compound fertilizer amount) in the North China Plain during 1987–2020; Data source: China Statistical Yearbooks 1979–2021. (B): the annual HONO emissions from fertilized fields in 2020 in China (0.68% of applied nitrogen was lost via HONO).